Enhanced Power Factor in Nanocomposite Chalcogenides

J. Martin, A. Datta, H. Kirby, A. Popescu, L.M. Woods, N. Crane and G.S. Nolas

Department of Physics, University of South Florida
Tampa, Florida, USA

USAMRMC

Marlow Industries

GM

U.S. Department of Energy
Energy Efficiency and Renewable Energy

2009 DOE Thermoelectric Applications Workshop

Novel Materials Laboratory
University of South Florida

How can we increase ZT?

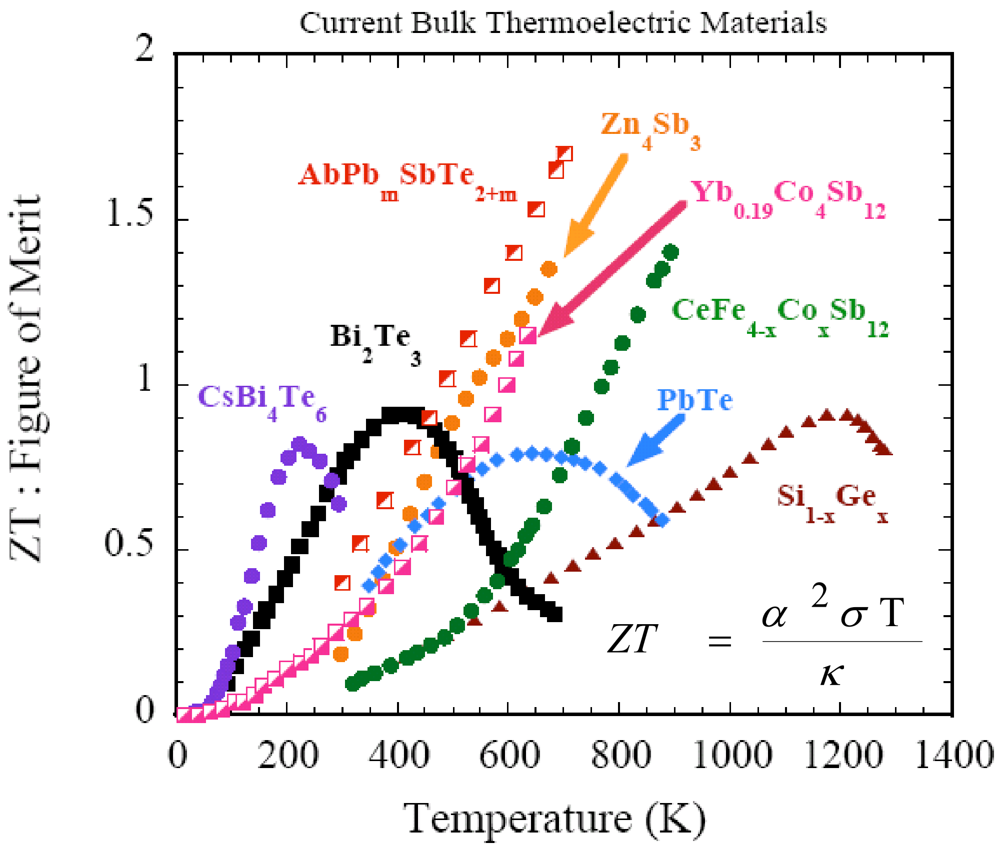

T.M. Tritt and M.A. Subramanian,
MRS Bulletin **31**, 188 (March 2006)

Thus far two approaches have shown the greatest promise:

1. **Phonon-Glass Electron-Crystal (*G. Slack*)**
2. **Low Dimensional Materials (*M. Dresselhaus*)**

TE Enhancement : Nanostructured Materials

- **Multilayered Structures first proposed in 1987[A]**
- **One dimensional quantum wires[B]**
- **Bi_2Te_3/Sb_2Te_3 supperlattice: ZT=2.4[C]**
- **Quantum dot supperlattice: ZT =1.6[D]**
- **Metal-based supperlattices[E]**

- **$Ag_mPb_mSbTe_{m+2}$ with nanoscale PbTe[2]: κ reduction**
- **Nanostructured SiGe bulk alloys[3]: κ reduction**
- **Nanostructured Bi_2Te_3 bulk alloys[4]: κ reduction**
- **Nanocrystalline $CoSb_3$[5]: κ reduction**
- **PbTe with Pb nanoprecipitates[6] : S increase**
- **PbTe nanocomposites[7, 8]: S increase**
- **PbTe 'dimensional' nanocomposites[9, 10]: S increase**

[A] T.E. Whall, *Proc. First Eur. Conf. on Therm.*, D.M. Rowe (Peter Peregrinus Lt., London, 1987)
[B] L.D. Hicks & M.S. Dresselhaus, PRB **47**, 16631 (1993)
[C] R. Venkatasubramanian et al, Nature **413**, 597 (2001)
[D] O.L. Lazarenkova & A.A. Balandin, PRB **66**, 245319 (2002)
[E] D. Vashaee and A. Shakouri, PRL **92**, 106103 (2004)

[1] K.F. Hsu *et al*, Science **303**, 818 (2004)
[2] G. Joshi *et al*, Nano Lett. **8**, 4670 (2008)
[3] M.S. Toprak *et al*, Adv. Func. Mat. **14**, 1189 (2004)
[4] B. Poudel *et al*, Science **320**, 634 (2008)
[5] X. Ji, T.M. Tritt *et al*, Phys. Stat. Sol. RRL **1**, 229 (2009)
[6] J.P. Heremans *et al*, JAP **98**, 063703 (2005)
[7] J.P. Heremans *et al*, Phys. Rev. B **70**, 115334 (2004)
[8] K. Kishimoto *et al*, JAP **92**, 2544 (2002)
[9] J. Martin *et al*, Appl. Phys. Lett. **90**, 222112 (2007)
[10] J. Martin *et al*, Phys. Rev. B **79**, 115311 (2009)

'Dimensional' Nanocomposites

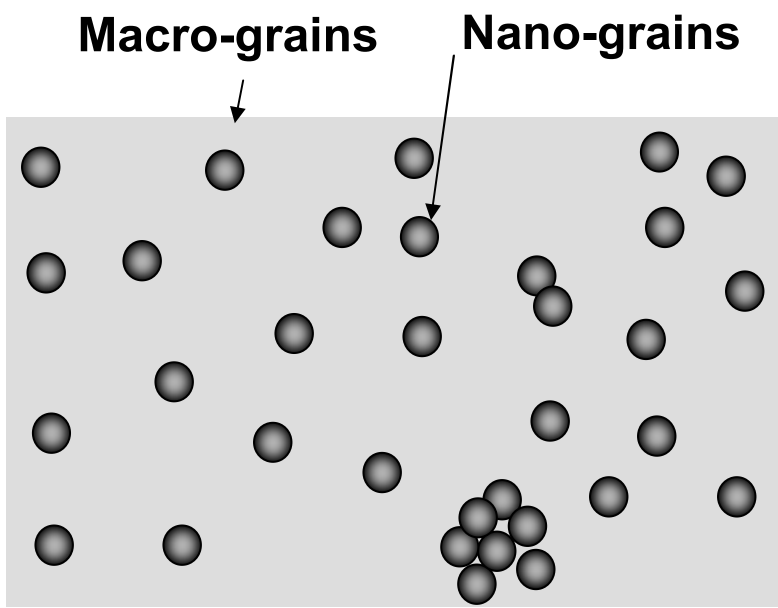

Expectations:
- Reduced thermal conductivity?
- Enhanced thermopower?
- Increased ZT?
- Cheap, self-assembly method

First Steps:
- Synthesis of high yield nanocrystals
- Densify into nanocomposites
- Measure transport properties

Lead Chalcogenides

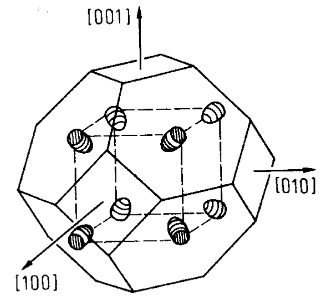

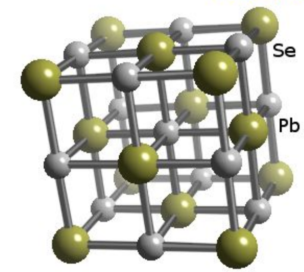

PbS, PbSe and PbTe

- NaCl-like FCC lattice structure
- Relatively low thermal conductivity
- Direct-gap semiconductor at the *L*-point of the Brillouin zone
- Bandgap between conduction and valence bands: PbS > PbTe > PbSe
- Lattice parameter: PbS < PbSe < PbTe

$$\frac{\hbar^2 k_l^2}{2m_l^*} + \frac{\hbar^2 k_t^2}{2m_t^*} = E + E^2 / E_g$$

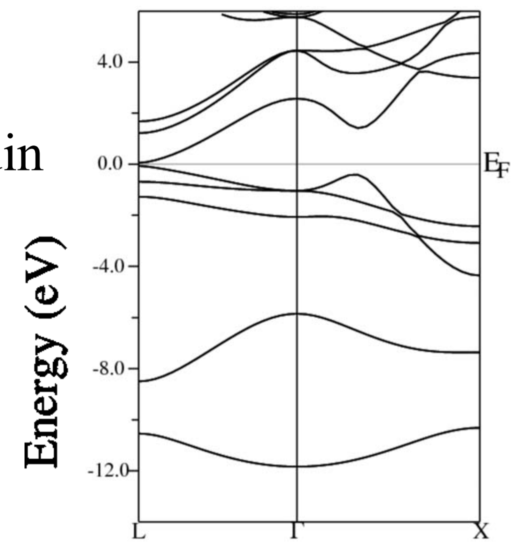

PbTe energy bandstructure

Bulk Property	PbS	PbSe	PbTe
Lattice Parameter (Å)	5.94	6.12	6.46
E_g at 77 K (meV)	307	168	215

X. Gao and M.S. Daw, Phys Rev B **77**, 033103 (2008)

Requirement: High Yield Nanocrystal Synthesis

Scalable!

NOVEL MATERIALS LABORATORY
UNIVERSITY OF SOUTH FLORIDA

PbTe Nanocomposites

Size & Shape Selectivity

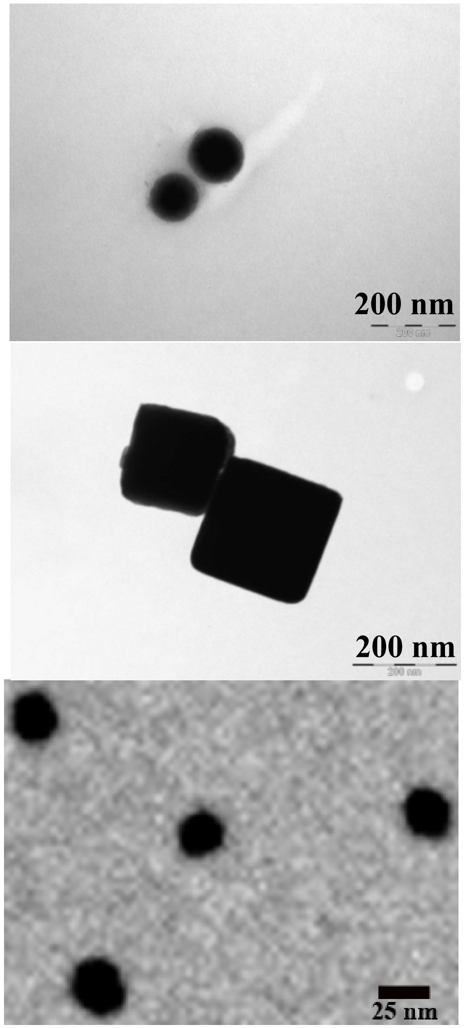

SPS

Densification

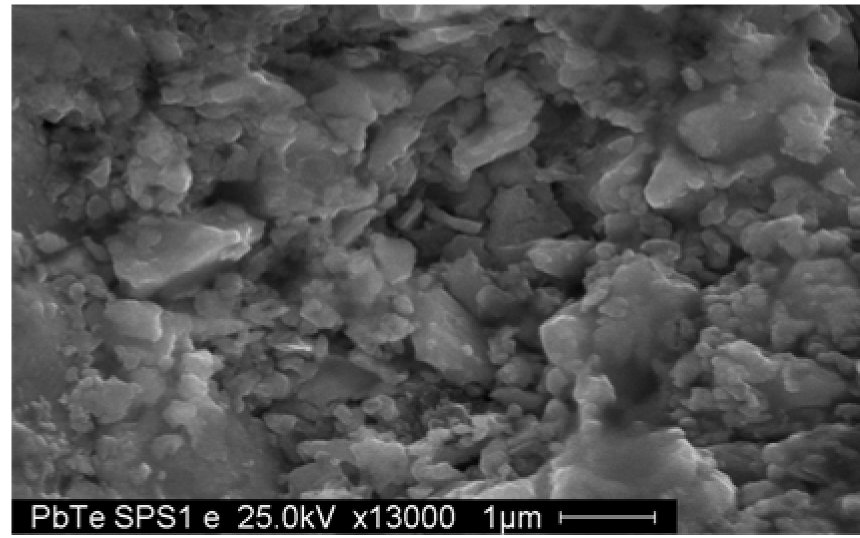

PbTe nanocrystals within the bulk matrix

J. Martin, G. S. Nolas, W. Zhang, and L. Chen, Appl. Phys. **90**, 222112 (2007)
J. Martin, L. Wang, L. Chen, and G.S. Nolas, Phys. Rev. B **79**, 115311 (2009)

Spark Plasma Sintering

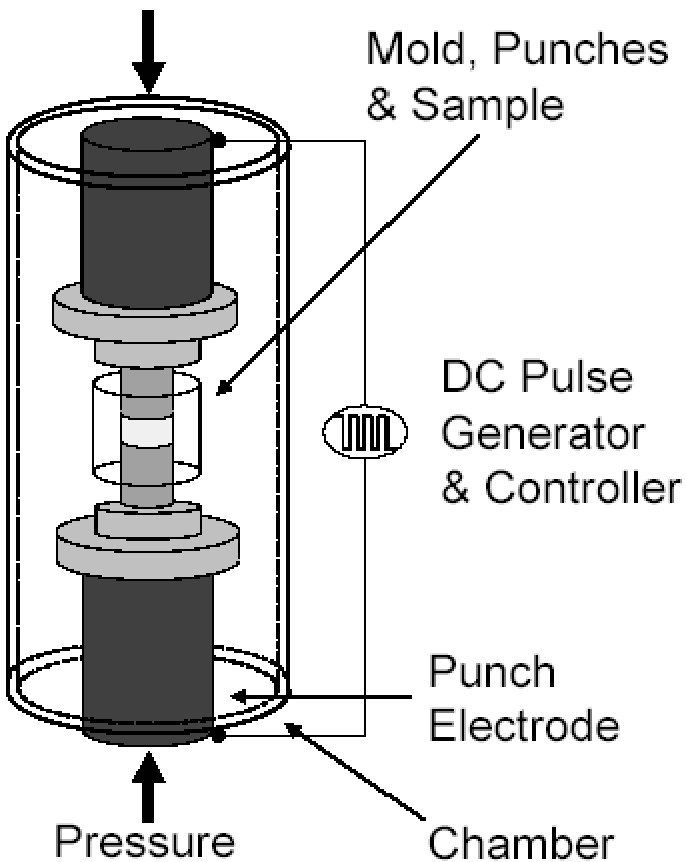

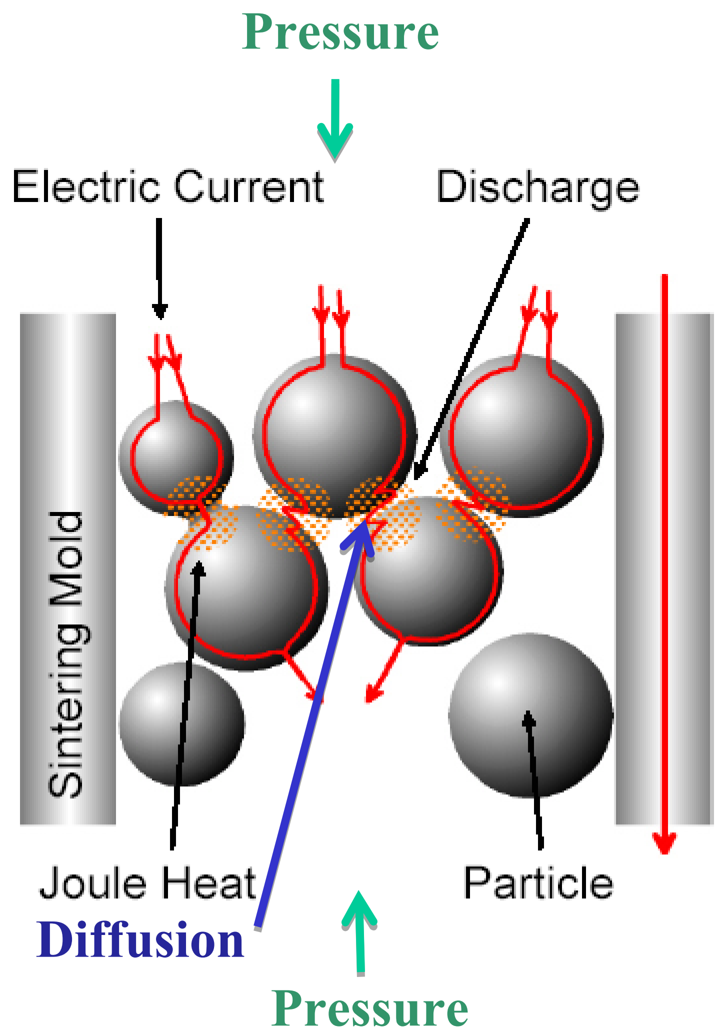

Powder and Polycrystalline XRD

PbTe

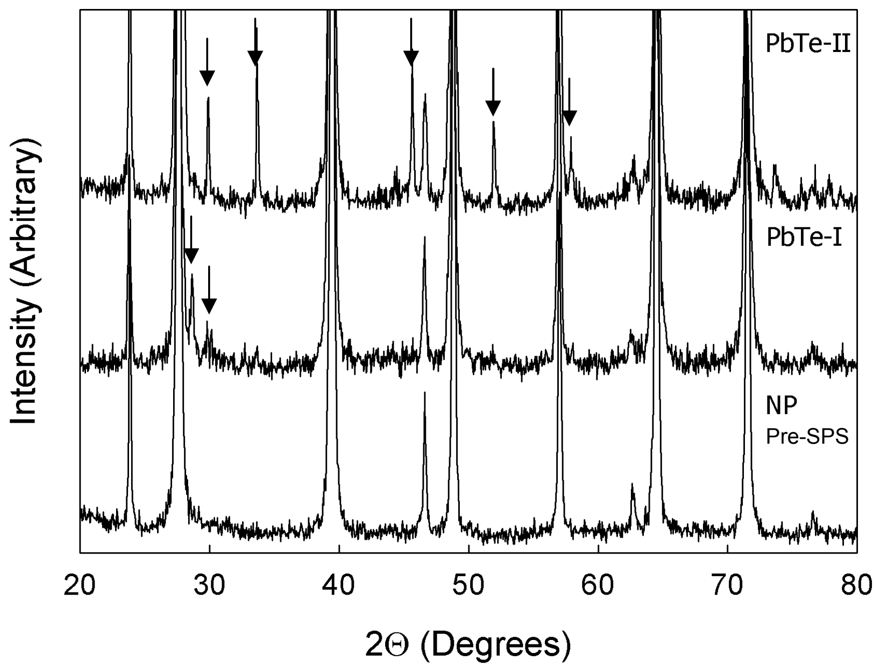

$PbTeO_3$ impurity

Ag-doped PbTe

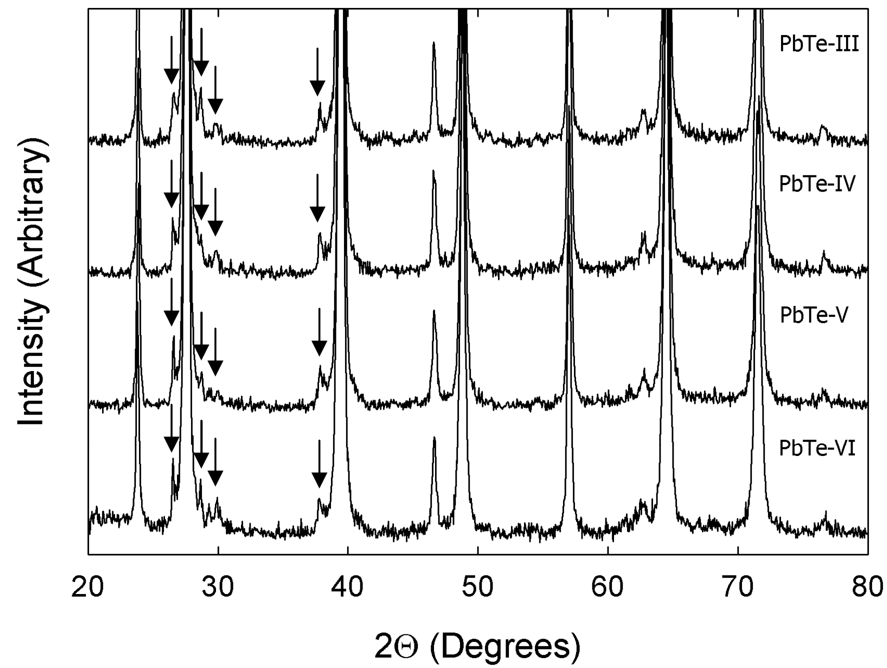

TeO_2 impurity

J. Martin, G. S. Nolas, W. Zhang, and L. Chen, Appl. Phys. **90**, 222112 (2007)
J. Martin, L. Wang, L. Chen, and G.S. Nolas, Phys. Rev. B **79**, 115311 (2009)

Novel Materials Laboratory
University of South Florida

PbTe Nanocomposites

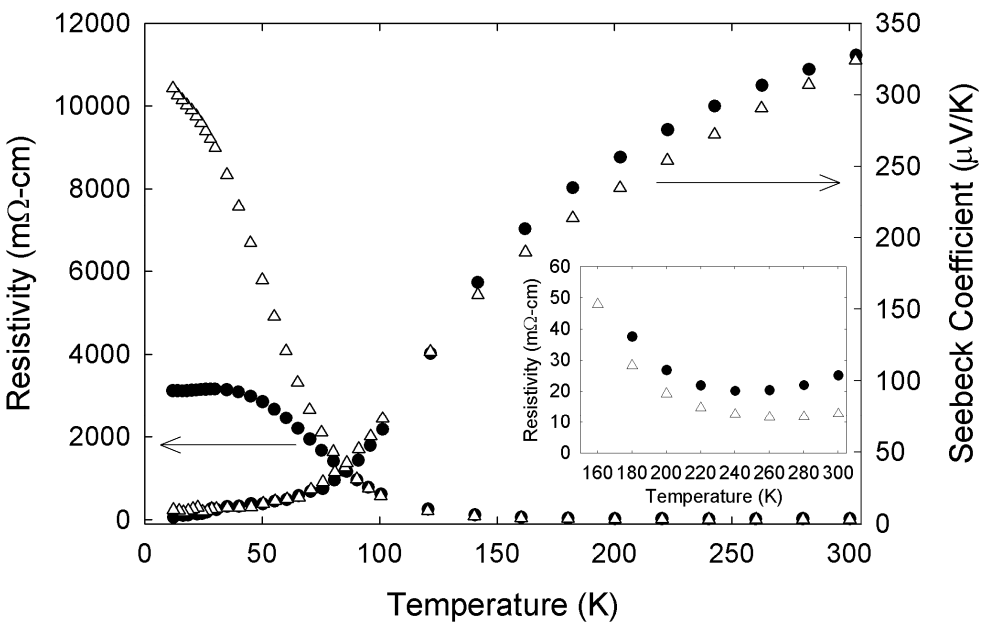

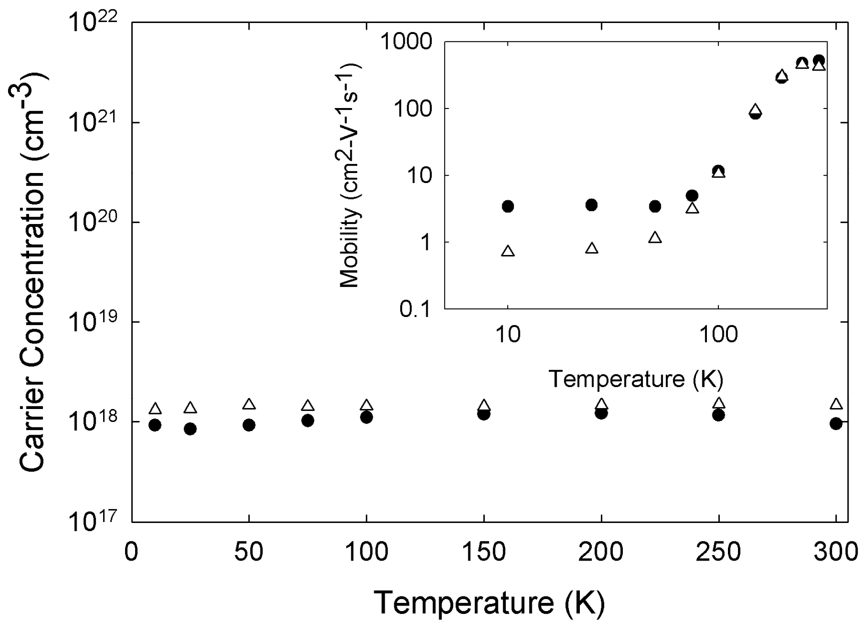

@ 300 K

Specimen	D (%)	ρ (mΩ-cm)	S (μV/K)	κ (W-m^{-1}K^{-1})	p (cm^{-3})	$S^2\sigma$ (μW/K^{2}cm)	Pb:Te
PbTe-I ●	94	24.9	328	2.2	9.5×10^{17}	4.3	49.91 : 50.09
PbTe-II △	95	12.6	324	2.5	1.5×10^{18}	8.3	50.42 : 49.58
B-I Bulk	97	37	325	-	8.0×10^{17}	2.9	-
B-II	97	19	250	-	9.5×10^{17}	3.3	-

J. Martin, G. S. Nolas, W. Zhang, and L. Chen, Appl. Phys. **90**, 222112 (2007)

PbTe Nanocomposites

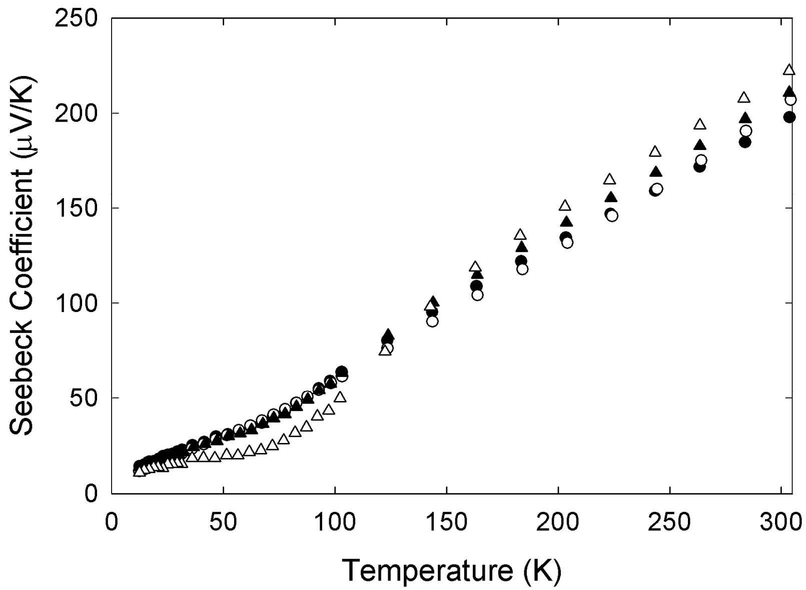

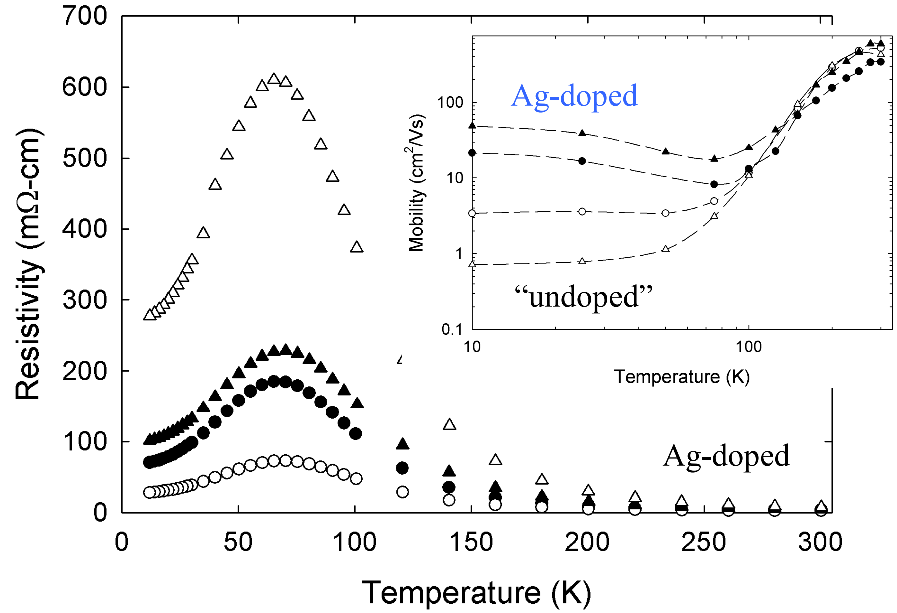

@ 300 K

Specimen	D (%)	ρ (mΩ-cm)	S (μV/K)	κ (W-m^{-1}K^{-1})	p (cm^{-3})	$S^2\sigma$ (μW/K^{2}cm)	Pb:Te
PbTe-I	94	24.9	328	2.2	9.5×10^{17}	4.3	49.91 : 50.09
PbTe-II	95	12.6	324	2.5	1.5×10^{18}	8.3	50.42 : 49.58
PbTe-III	95	3.9	198	2.8	5.1×10^{18}	10.0	-
PbTe-IV	94	2.9	207	2.7	6.2×10^{18}	14.8	-

J. Martin, L. Wang, L. Chen, and G.S. Nolas, Phys. Rev. B **79**, 115311 (2009)

Novel Materials Laboratory
University of South Florida

Thermopower Enhancement in Nanocomposites

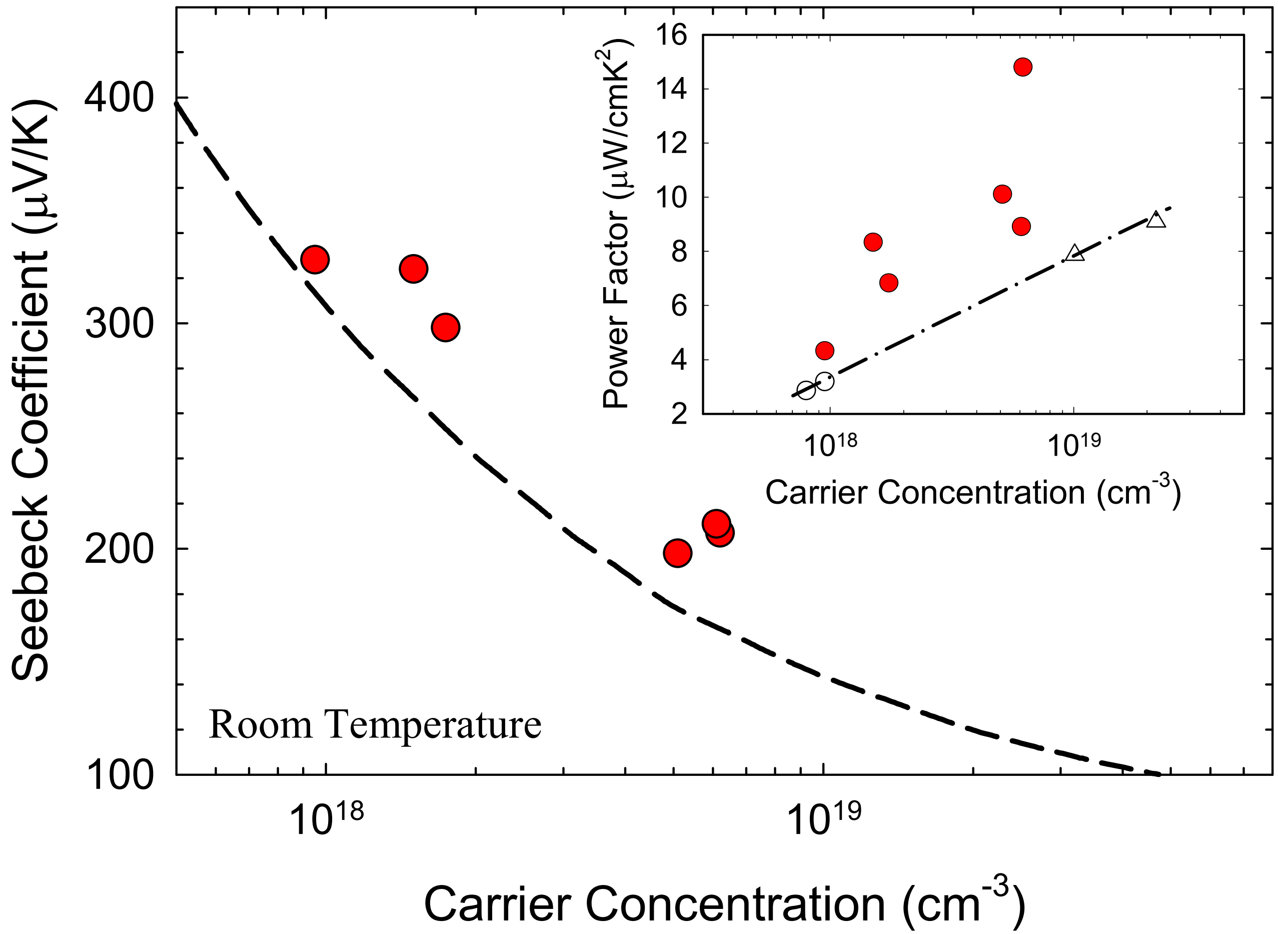

red PbTe Nanocomposites △, ○ Bulk PbTe

- - - - A.J. Crocker *et al*., Brit. J. Appl. Phys. **18**, 563 (1967)

H. Kirby, J. Martin, L. Chen, and G.S. Nolas, Proc. Mater. Res. Soc. **1166** (2009)

PbTe Nanocomposites

$$\mu_{eff} = Lq\left(\frac{1}{2\pi m^* kT}\right)^{1/2} \exp\left(-\frac{E_B}{kT}\right)$$

Density of trapping states: $E_B = \frac{q^2 N_t^2}{8\varepsilon\varepsilon_o p}$

Width of space-charge region: $W = \left(\frac{2\varepsilon\varepsilon_o E_B}{q^2 p}\right)^{1/2}$

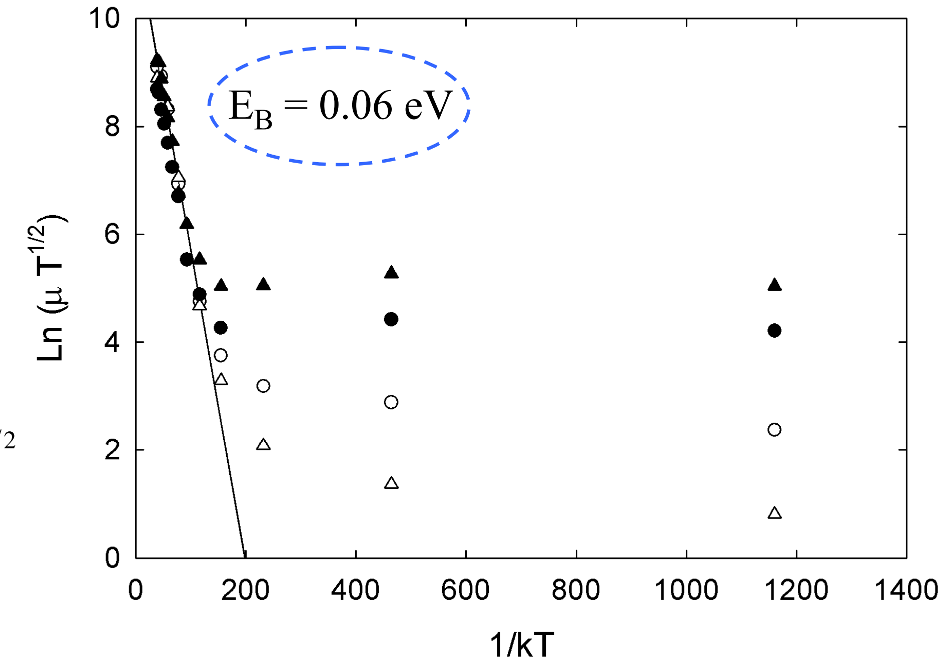

@ 300 K

Specimen	ρ (mΩ-cm)	p (cm^{-3})	E_B (meV)	N_t (cm^{-2})	W (nm)	L (nm)
PbTe I ○	24.9	9.5 x 10^{17}	60	1.0 x 10^{13}	54	316
PbTe II △	12.6	1.5 x 10^{18}	60	1.3 x 10^{13}	43	396
PbTe III ●	3.9	5.1 x 10^{18}	60	2.4 x 10^{13}	23	376
PbTe IV ▲	2.9	6.2 x 10^{18}	60	2.6 x 10^{13}	21	416

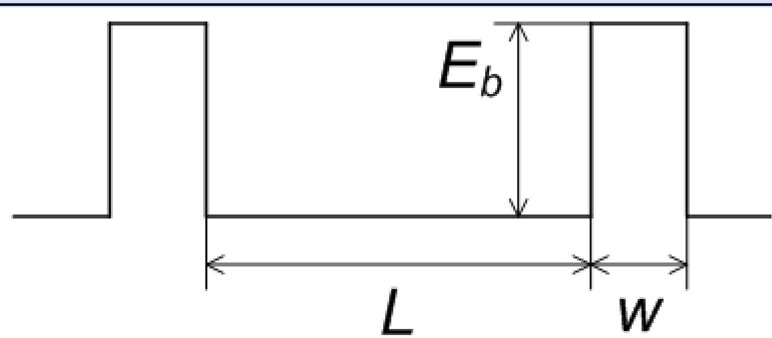

C. H. Seager, J. Appl. Phys. **52**, 3960 (1981)
O. Vigil-Galan, J. Appl. Phys. **90**, 3427 (2001)
J. Y. W. Seto, J. Appl. Phys. **46**, 5247 (1975)

Model : Granular Nanocomposites

Goal **- describe electrical conductivity and Seebeck coefficient**
- understand the role of grain interface scattering

$$\sigma = \frac{2e^2}{3m^*}\int_0^\infty \tau(E)g(E)E\left(-\frac{\partial f(E)}{\partial E}\right)dE$$

$$S = \frac{1}{eT}\left[\frac{\int_0^\infty \tau(E)g(E)E^2\left(-\frac{\partial f(E)}{\partial E}\right)dE}{\int_0^\infty \tau(E)g(E)E\left(-\frac{\partial f(E)}{\partial E}\right)dE} - \mu\right]$$

e – electron charge
m^* - effective mass
T – temperature
μ – chemical potential

$\tau(E)$ – relaxation rate
$g(E)$ – total density of states (DOS)
$f(E)$ – energy distribution function

diffusive, quasi-equilibrium transport
σ, S – derived using linear response theory

A. Popescu, L.M. Woods, J. Martin, and G.S. Nolas, Phys. Rev. B **79**, 305302 (2009)

Scattering Mechanisms

$$\frac{1}{\tau(E)} = \sum_n \frac{1}{\tau_n(E)}$$

Scattering due to acoustic phonons

$$\tau_{a-ph}(E) = \frac{h^4}{8\pi^3} \frac{\rho v_L^2}{k_B T} \frac{1}{(2m^*)^{3/2} D^2} E^{-1/2}$$

Scattering due to optical phonons

$$\tau(E)_{o-ph} = \frac{h^2}{2^{1/2} m^{*1/2} e^2 k_B T(\varepsilon_\infty^{-1} - \varepsilon_0^{-1})} E^{1/2}$$

Scattering due to ionized impurities

$$\tau_{imp}(E) = \left[\frac{Z^2 e^4 N_i}{16\pi(2m^*)^{1/2}\varepsilon^2} \ln\left[1 + \left(\frac{2E}{E_m}\right)^2\right]\right]^{-1} E^{3/2}$$

Interface grain barriers

$$\tau_b(E) = \lambda / v \qquad v = \sqrt{2E/m^*}$$

$$\lambda = \sum_{n=1}^{\infty} T^n(E)(1-T(E))nL = \frac{T(E)L}{1-T(E)}$$

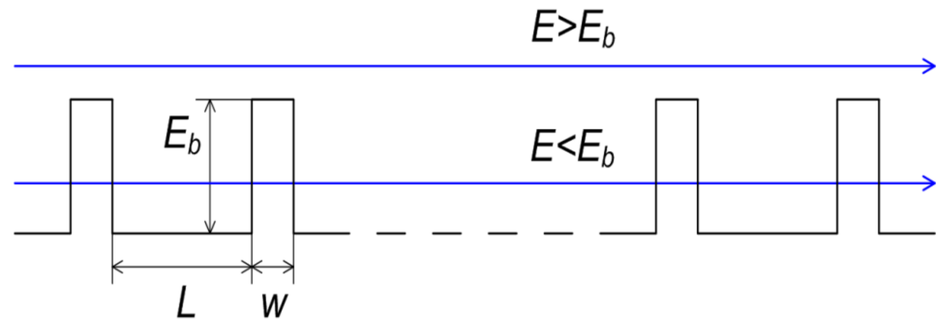

Infinite number of barriers:
E_b – barrier height
w – barrier width
L – distance between the barriers
$T(E)$ – quantum mechanical transmission through one barrier

ρ – mass density
v_L – longitudinal speed of sound
D – deformation potential constant
N_i – concentration of impurities
$\varepsilon_{0,\infty}$ - dielectric constants

Comparison: Experiment and Theory

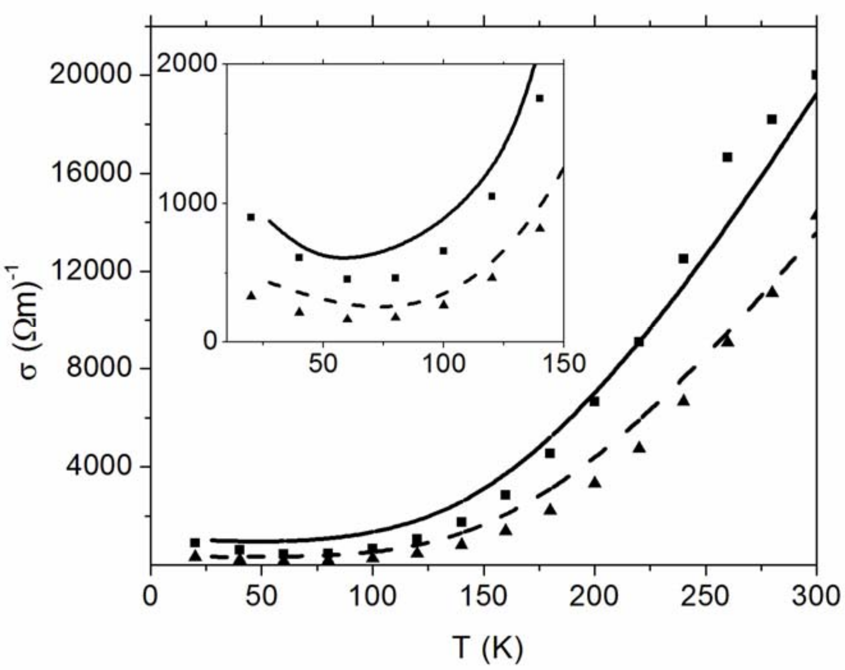

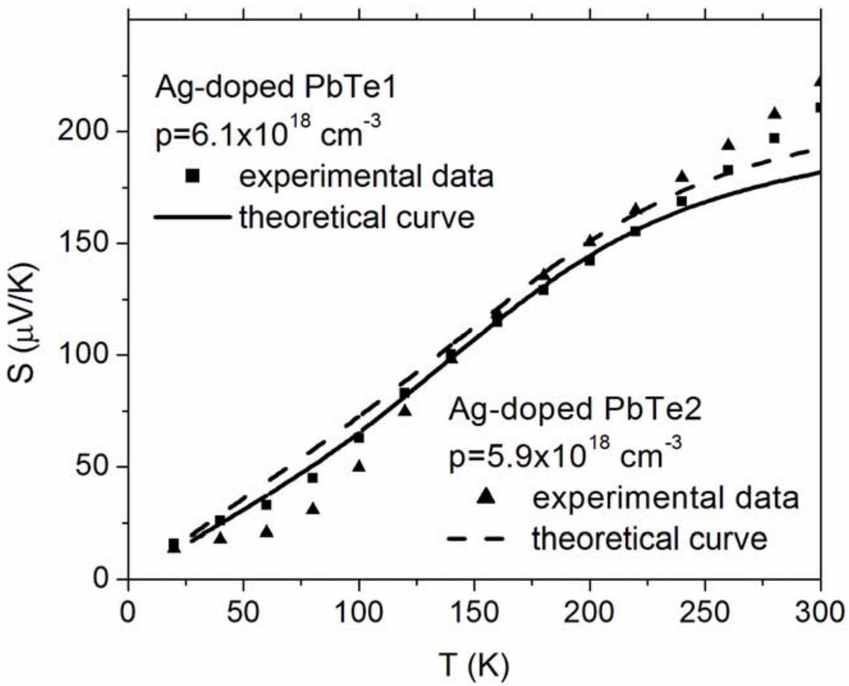

comp	***ρ (g/cm³)***	***v_L (m/s)***	***D (eV)***	***m^*/m_0***	***ε_∞^{-1}-ε_0^{-1}***
PbTe	8.16	1730	5 – 15	0.16	0.0022

A. Popescu, L.M. Woods, J. Martin, and G.S. Nolas, Phys. Rev. B **79**, 305302 (2009)

TE Transport Properties:
The role of Carrier Concentration

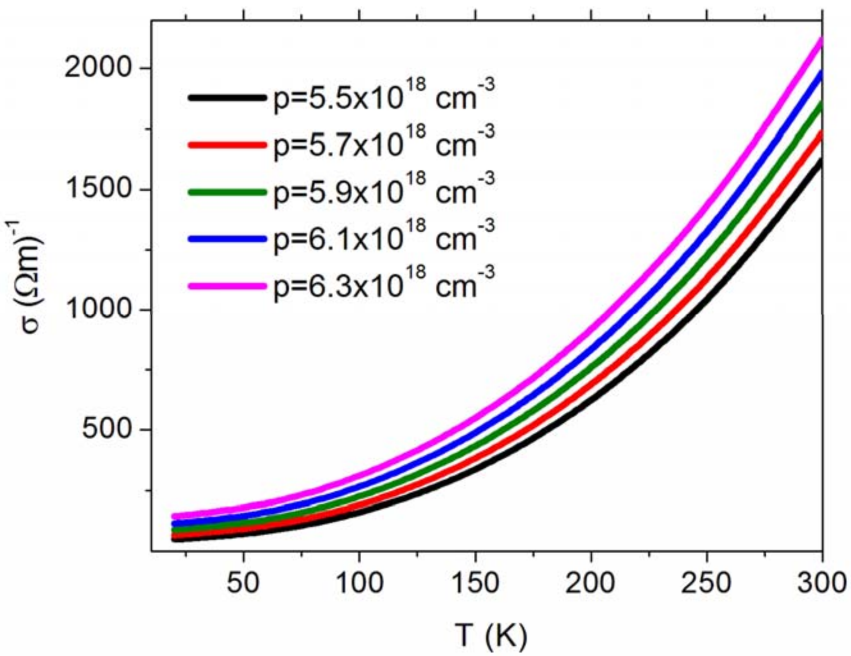

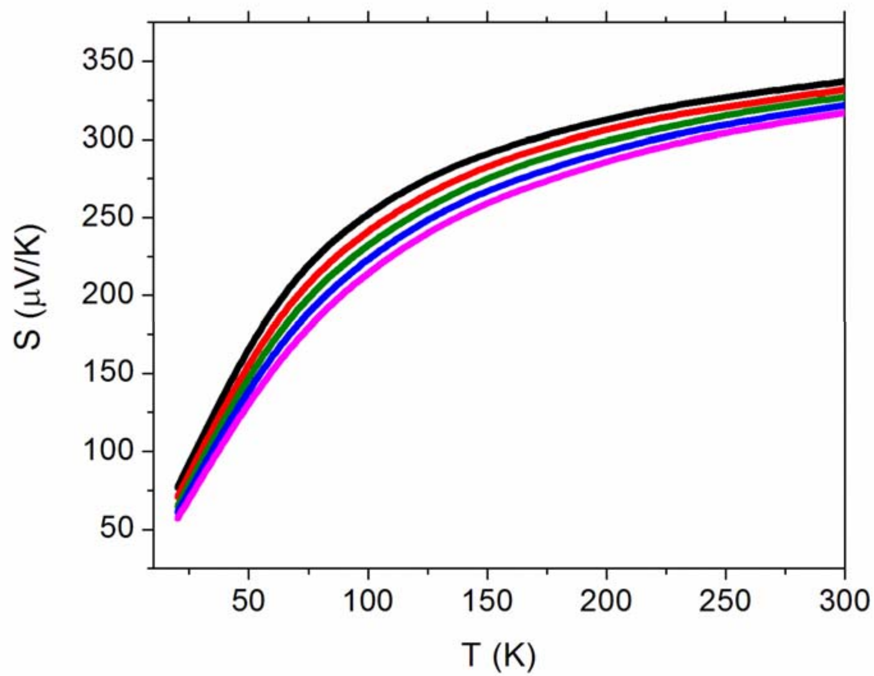

Higher concentration results in more transport carriers → ***σ increases & S decreases.***

Novel Materials Laboratory
University of South Florida

Grain Boundary Height

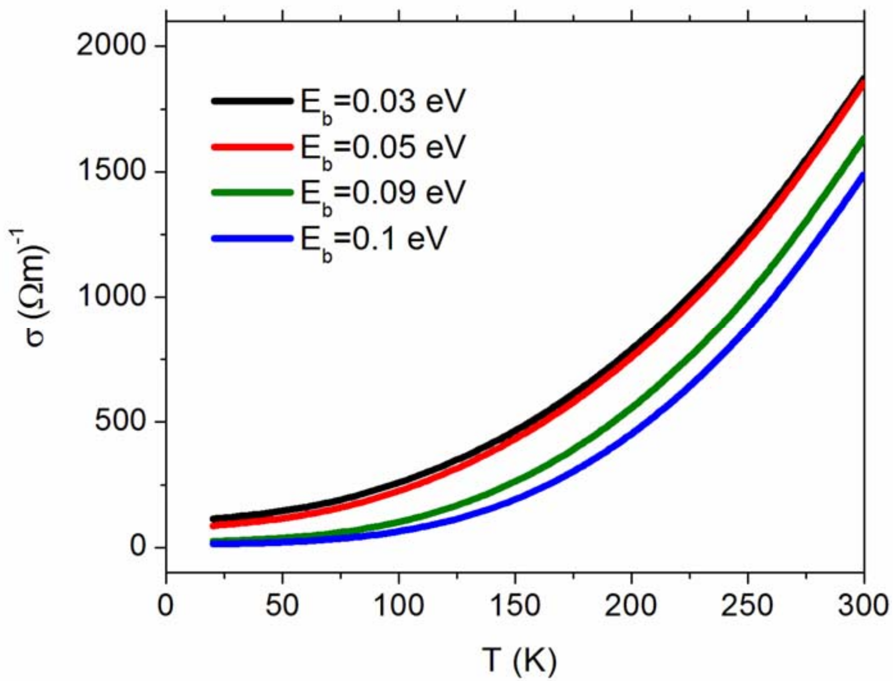

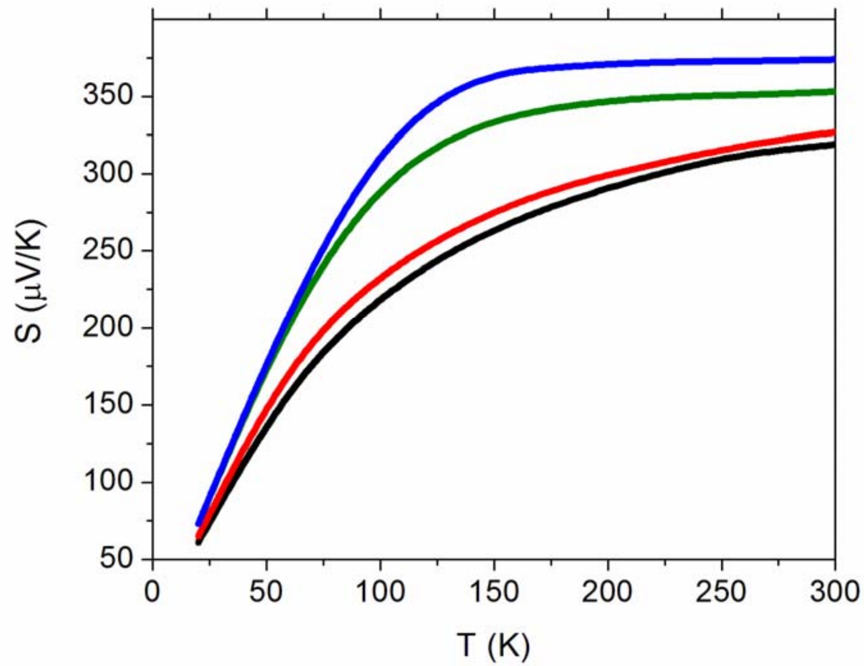

Higher E_b – more carriers are scattered → ***σ decreases & S increases***

Lower E_b – carrier energy larger than barrier → ***σ increases & S decreases***

Grain Boundary Width

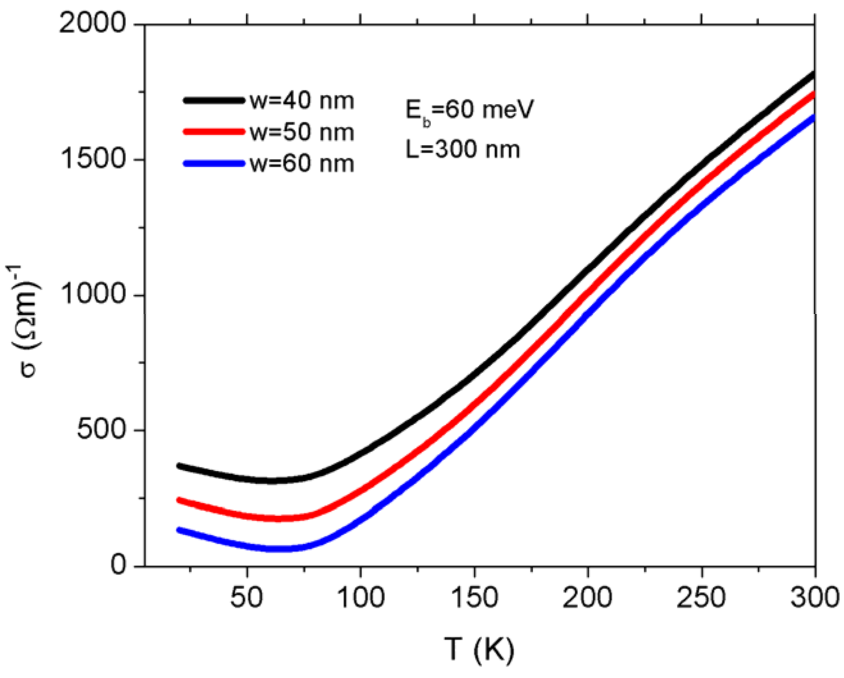

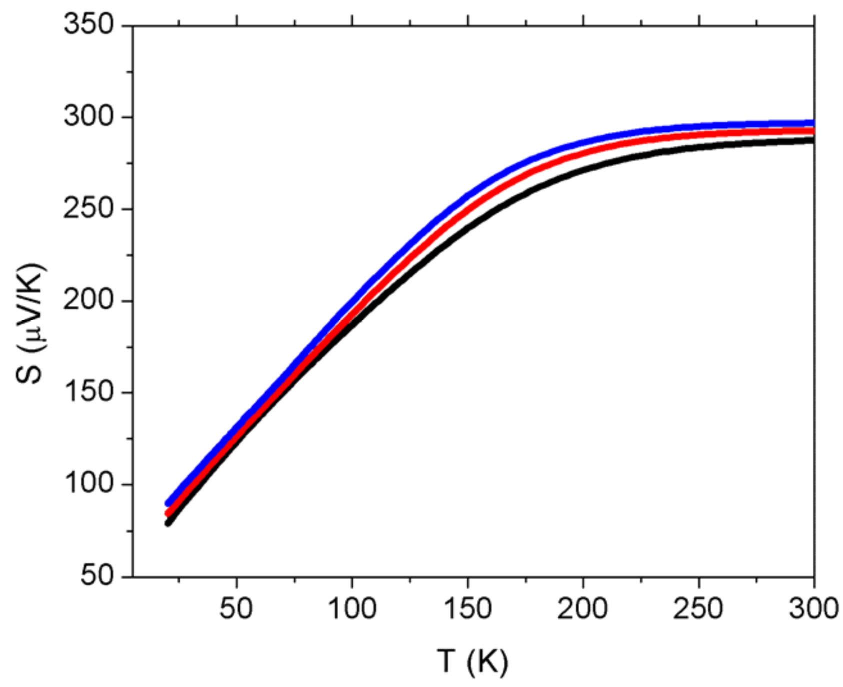

Larger w – smaller transmission probability T(E) → ***σ decreases & S increases***

Smaller w – larger transmission probability T(E) → ***σ increases & S decreases***

Distance (*L*) Between Barriers

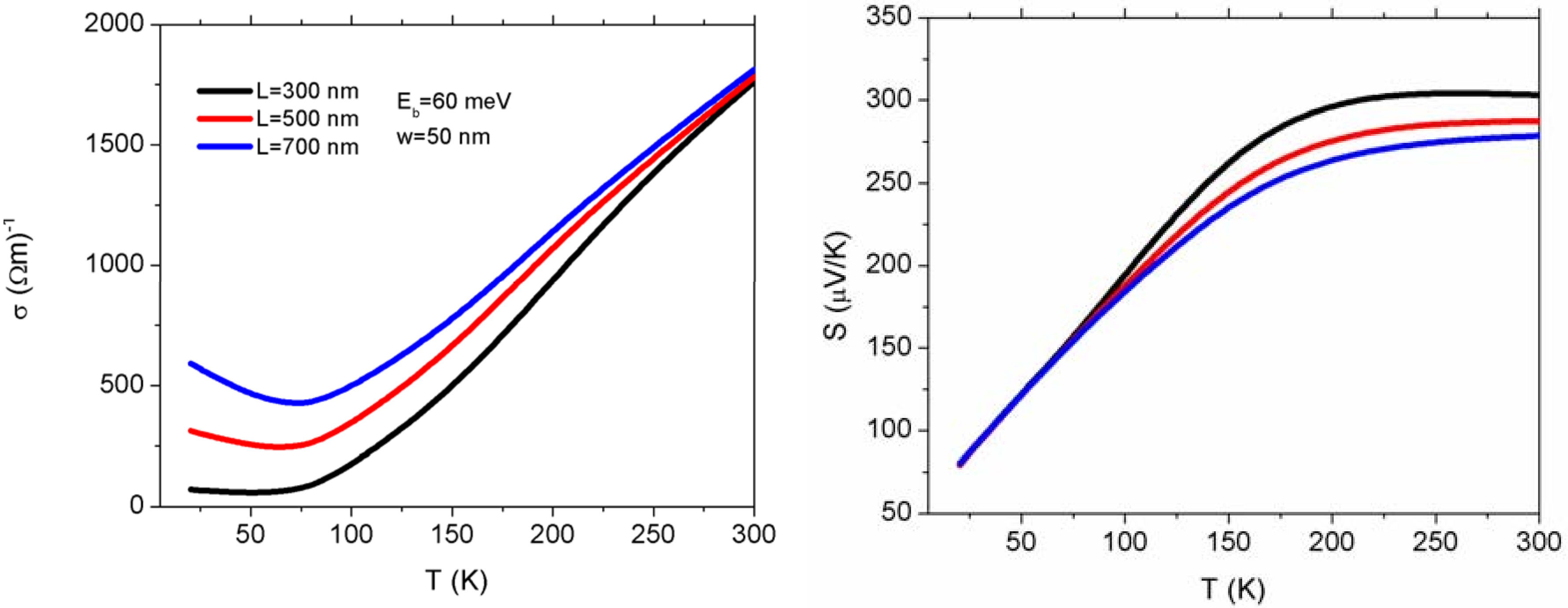

Smaller L – more frequent carrier/interface scattering → ***σ decreases & S increases***

Larger L – less frequent carrier/interface scattering → ***σ increases & S decreases***

$S^2\sigma$ for PbTe granular nanocomposites

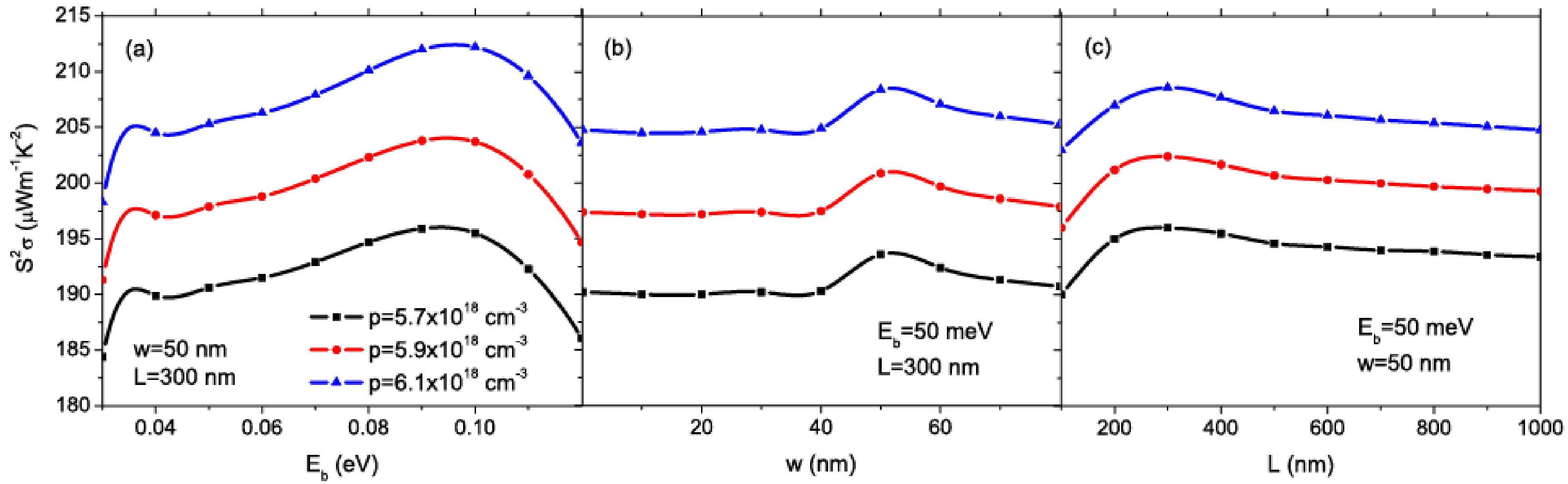

A. Popescu, L.M. Woods, J. Martin, and G.S. Nolas, Phys. Rev. B **79**, 305302 (2009)

Novel Materials Laboratory
University of South Florida

$CoSb_3$ for PbTe granular nanocomposites

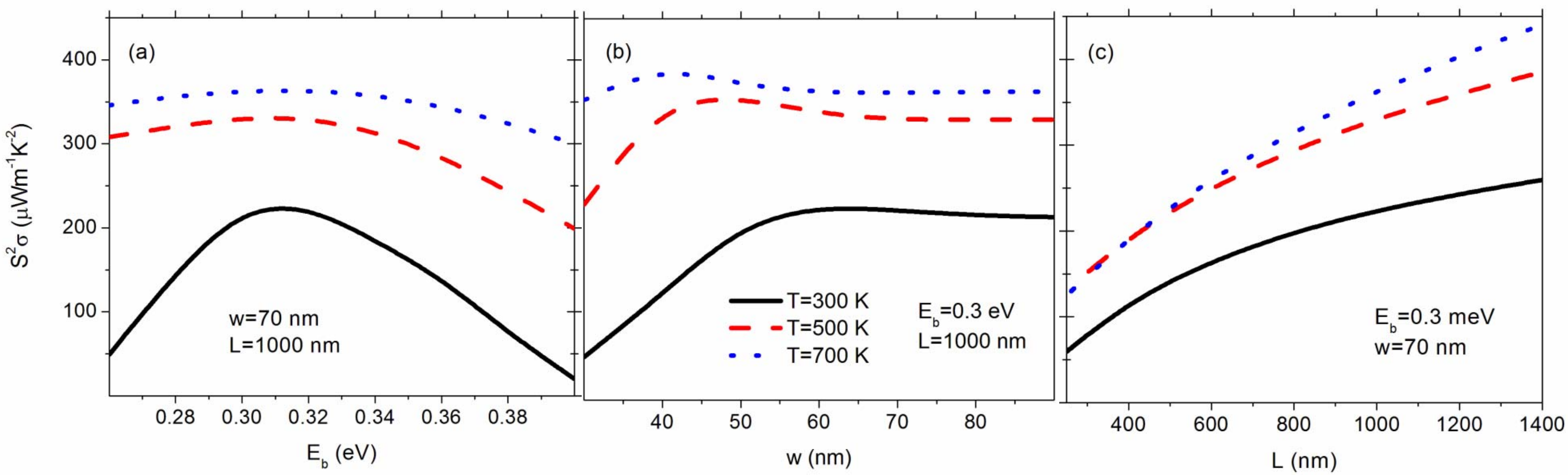

L.M. Woods, A. Popescu, J. Martin, and G.S. Nolas, Proc. Mater. Rec. Soc. **1166** (2009)

Device manufacturing: Self Assembly

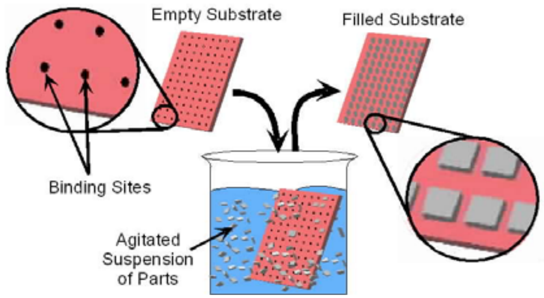

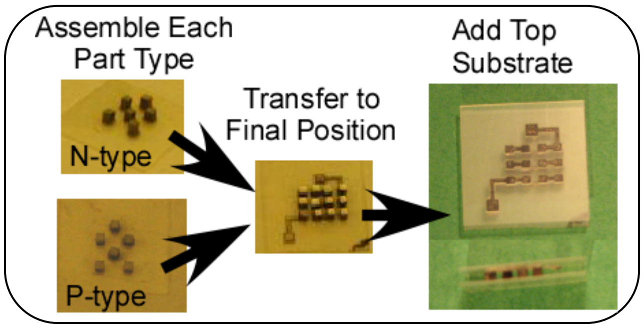

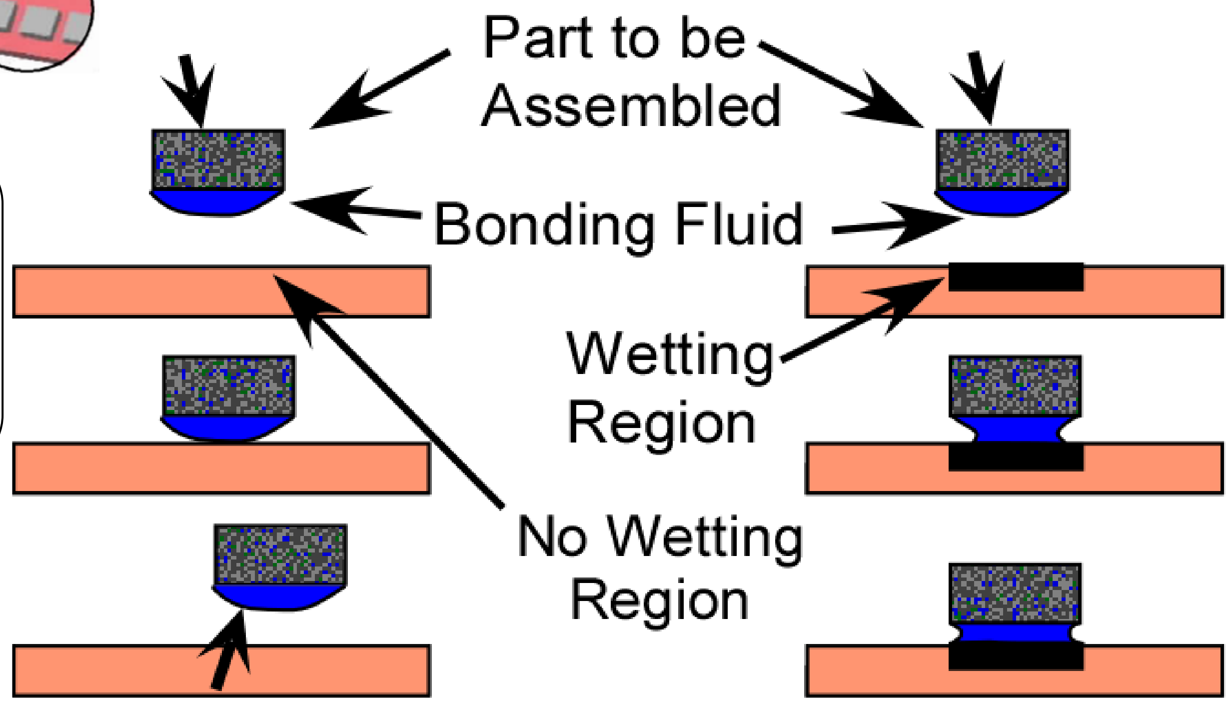

Challenge of Self Assembly: Rate & Yield

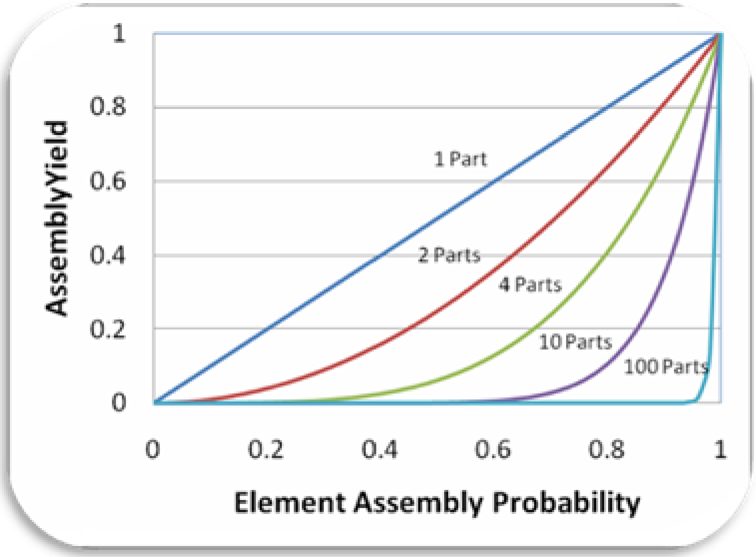

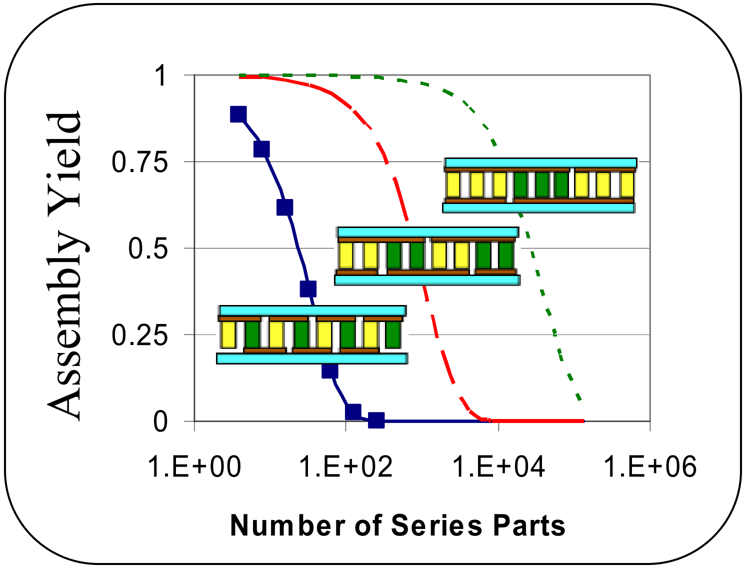

Assembly yield depend on process and design parameters.

Goal: Develop predictive models of self assembly process rate and yield to facilitate design of high rate and yield processes at industrial scales.

N. Crane, P. Mishra, J. Murray, G.S. Nolas, J. Electronic Mater **38**, 1252 (2009)

Novel Materials Laboratory
University of South Florida

Acknowledgements

Lidong Chen

Shanghai Institute of Ceramics, China

Jim Salvador & Jihui Yang

General Motors Co. Inc., USA